Charles University in Prague
Faculty of Science
Department of Analytical Chemistry

SUMMARY OF PhD THESIS

Material Research of Colour Layer in Artworks

Ph.D. programme: Analytical Chemistry

Ing. Veronika Grünwaldová

Prague 2010

CONTENTS

Introduction and literature search

The introductory part of the thesis is devoted to the literature search comprising about 180 references to scientific literature, dating mainly from the last ten years. This search maps contemporary methods for material research of artwork. Analytical methods standardly used in this field may be divided into four main groups. Microscopy methods are the most widespread methods (light and scanning electron microscopy- SEM), methods of element analysis constitute the second group (X-ray fluorescence spectrometry- XRF, energy dispersive- EDX /wavelength dispersive X-ray analysis- WDX), the third group is comprised of methods dealing with molecules and their structure (X-ray diffraction-XRD, molecular infrared spectroscopy, Raman spectrometry), and methods of isotope analysis used especially for dating and origin determination belong to the fourth group. Rarely, other analytical techniques are also used for artwork analysis, e.g. particle induced X-ray emission, laser induced breakdown spectroscopy, neutron activation analysis, nuclear magnetic resonance spectroscopy, small angle X-ray scattering, reflection spectroscopy or mass spectrometry. The principles of individual methods and examples of their use are briefly introduced in the literature search section.

The aim of this experimental work was to test newly developed selected methods for inorganic analysis of the colour layer of artwork, which would complement the current procedure of material research as much as possible.

Experimental section

Based on the complex literature search three areas of interest providing a marked progress in the current method of material research were chosen:

1) systematic testing and development of X-ray powder microdiffraction measurement technique for the analysis of artwork samples,
2) mathematical processing of microscope produced pictures using image analysis techniques,
3) comparison of two mobile X-ray fluorescence analyzers.

1. X-ray powder microdiffraction

With regard to the necessity of nondestructive phase analysis of small points the first area of interest of this thesis focused on testing and development of a method of measuring color layers of artworks using a new high-resolution method - X-ray powder microdiffraction an on its introduction to common practice of material research.

Microdiffraction experiments were performed using an instrument produced by a Dutch company, PANalytical X´PertPRO, which advantageously combines a common X-ray tube with a special mono-capillary and a very fast semiconductor detector. The mono-capillary is a hollow glass tube, in which the X-ray beam is completely reflected. The divergent X-ray beam becomes quasi-parallel, in our case, with a diameter of 100 μm at the end of the tube. In addition to collimation of the X-ray beam, the mono-capillary also serves as an energy filter and suppresses white radiation. The mono-capillary is optimized for Cu Kα radiation, but may also be used for other types of radiation, the energy of which is less than 10 keV, such as Cr, Fe, and also Co Kα. The position-sensitive detector X'Celerator provides direct detection of diffracted X-rays and is able to efficiently process the input signal without decreasing the quality of resolution.

1.1. Analysis of fragments and cross-sections

Gradually, a method for the analysis of standard samples of artworks – fragments and cross-sections was developed. X-ray powder microdiffraction has been successfully used in this testing for interpretation of the mineralogical composition of salt effloresces formed due to inconvenient environmental conditions or to careless or unprofessional restorer intervention on the surface of paintings. Further on, it was used for direct identification of a spectrum of inorganic pigments (azurite, Prussian blue, etc.) and for identification of the method of preparation of a medieval pigment – lead-tin yellow type I in the funeral crown of Charles IV. In addition, different types of colour grounds could also be successfully differentiated according to their origin. In all these cases it was necessary to use non-destructive direct phase analysis, as the chemical composition was insufficient for correct interpretation.

Comparison of measurement results in conventional and microdiffraction configuration has proven that powder X-ray microdiffraction is necessary to correctly interpret the composition of individual layers in the microsample. The following example shows that the layers of the microsample practically cannot be separated without a high risk of contamination. A sample taken from a mural painting in a convent in Plasy was divided into parts. From one part of the sample the green layer was carefully separated and, after homogenization, measured on a zero background silicon underpad with powder X-ray diffraction using conventional configuration. With this method celadonite and chlorite (Fig. 1.1) were detected in addition to calcite, gypsum, albite and quartz. Both of these minerals are of green color and were used as a pigment – referred to as “Green Earth”. Subsequent microdiffraction measurements were performed on the other portion of the taken sample, both right on the surface of the green layer of the fragment, and on a cross-section. Both microdiffraction measurements (Fig. 1.1), i.e. the fragment measurement and the cross-section measurement, however, confirmed in mutual accordance only the presence of celadonite. Thus, this finding lead to the hypothesis that chlorite was not used as a pigment in that case, but as a component of the plaster as a relatively common natural mineral, which got into the green layer due to its imperfect separation. Another interesting phenomenon observed during these measurements is the occurrence of gypsum (Fig. 1.1). Two different sources of gypsum were identified by comparing the relative representation of this phase in the powder, cross-section, and fragment. The small amount contained in the powder, an averaged sample, could indicate gypsum, the source of which was plaster. On the other hand, the highly elevated proportion on the fragment surface and its absence in the cross-section pigment layer indicate

that its origin should be found in so called salt efflorescence, i.e. corrosion damage to the mural.

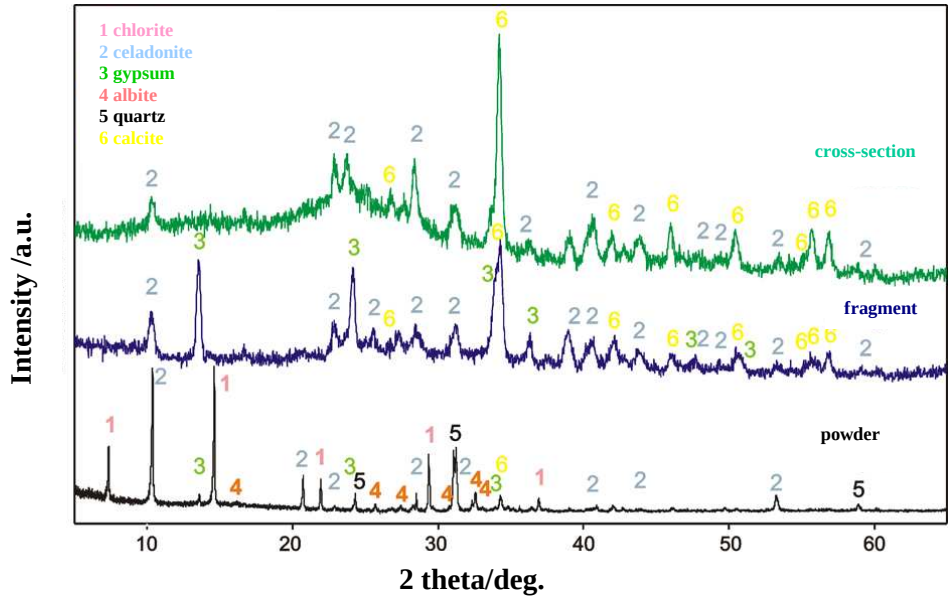

Fig. 1.1:Comparison of diffractograms of the cross-section, fragment and powder from a convent mural in Plasy.

1.2. Preparation and analysis of microtome slices

Besides testing the powder X-ray microdiffraction for the analysis of standard types of samples, the objective was to develop such a sample form, which could be used for X-ray microdiffraction, and also for other analytical techniques. The technique of microtome slices, which makes it possible to perform all the necessary analyses from one identical place of the microsample, seemed promising. Introducing this technique would eliminate the formerly common division of samples, which created the risk (due to inhomogeneity of the studied phases) that different methods might study different materials. Therefore, during the next phase, a technology of microtome slice preparation by microtome cutting from a cross-section was developed. An optimum embedding resin (Bylapox) and suitable cutting conditions, such as material and angle of the cutting knife (hard metal, 2° – 8°), or optimum slice thickness (5 –9 μm) were successfully detected to maximize the yield of quality slices. As the underpad for the slice a special zero background plate of monocrystalline silica cut at the level (100) was used. The advantage of this plate is the possibility of transferring the microtome slice into another instrument and its subsequent analysis by other analytical techniques, such as SEM/EDX or transmission infrared microscopy, without the necessity of any additional

sample adjustment. An example of microtome slice analysis of a real colour layer sample is given in Fig. 1.2.

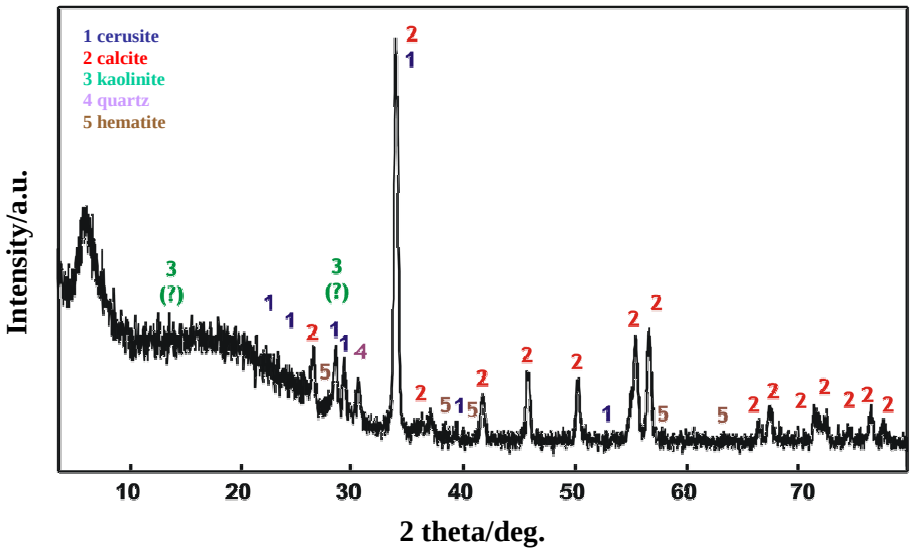

Fig. 1.2: Diffractogram of brown underlaying layer of sample J0534-7 slice.

However, detailed testing has shown that in the case of e.g. SEM/EDX analysis the microtome slice cannot fully replace the analysis of the cross-section across the color layers of the sample. The risk that important layers are not conserved or are overlooked is relatively high.

An attempt to estimate the detection limit for identification of crystalline phases formed by light elements (organic pigment indigo, clay mineral kaolinite) in a microtome slice was performed on a model sample of blue pigments. The limit was roughly set at 5 mass percent.

2. Microscopy methods and image analysis

The second thematic focus of the thesis was dealing with the mathematical processing of image data yielded by commonly used microscopy techniques. Even though correct reading and processing of image information is crucial for other procedures, the methods of image analysis by means of mathematical processing of image information, have not been included in material research of artwork practically anywhere so far.

Out of a large amount of parameters, which may be monitored by image analysis, namely the parameters characterizing shape and size, eventually parameters of orientation within the layers of the painting, are significant for characterization of color layer particles. To express the particle size distribution, the morphological parameters and maximum and

minimum Feret diameter appeared to be optimal. Particle perimeter and area are parameters related to both the shape and size of particles. Particle shapes are well characterized by morphological parameters, elongation and circularity. For the purposes of this study an image analysis program NIS ELEMENTS 3.1. and Lucia G version 4.71. [172] were used.

2.1. Test of minimum necessary resolution – model shapes and real samples

Correct mathematical characterization of particle size and shape depends on the quality of the source image data. Therefore, a test to determine the minimum necessary resolution of the used microphotographs was performed first. Using models in the shape of a circle, five pointed star and twelve pointed star, which simulates varying degrees of complexity, it was found that for elementary **object size** detection a minimum resolution of 8x8 pixels **per one object/particle** of the sample is sufficient. To characterize morphological parameters of **object shape** it is necessary to use resolutions of 64 x 64 pixels to 128x128 – according to shape complexity **per one object**.

Through subsequent tests of microphotographs of real samples of color layers, which usually contain hundreds to thousands of different objects in one photograph, it was found that for a meaningful characterization of such a number of objects in one image the minimum necessary resolution is 1024x1024 to 1200x1200 image points for the measured field. This reasoning applies in the case of magnification, which corresponds to the above mentioned covering of particles by image points and for the size span of particles common in color layers (i.e. ~ 1 –100 μm). An example of a change in the appearance of microphotograph of a real color layer taken at the resolution of 64x64 pixels and 2048x2048 pixels is documented in Figure 2.1a and 2.1b.

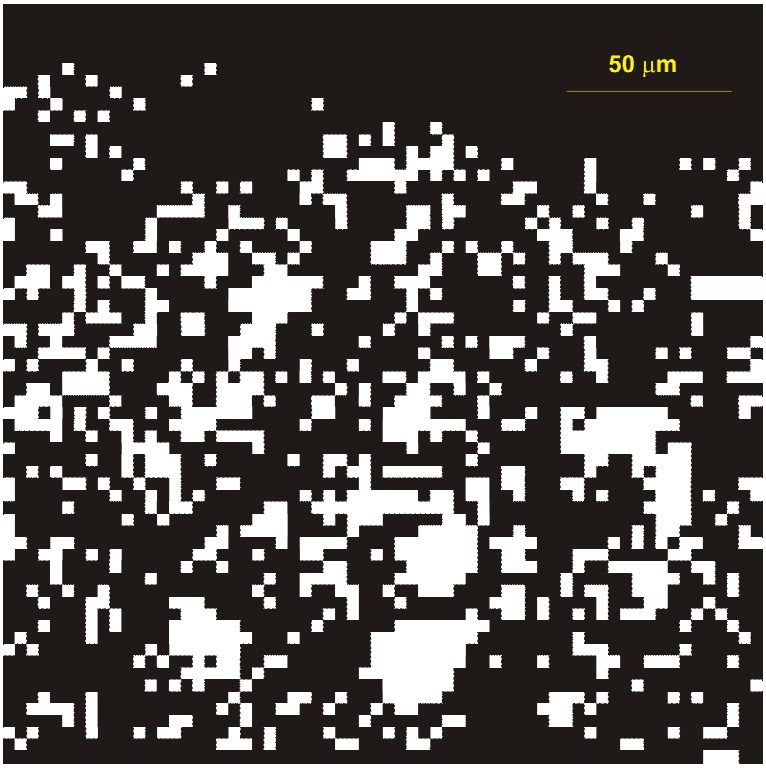

Fig. 2.1a: SEM image of a real sample recorded at the resolution of 64x64 pixels.

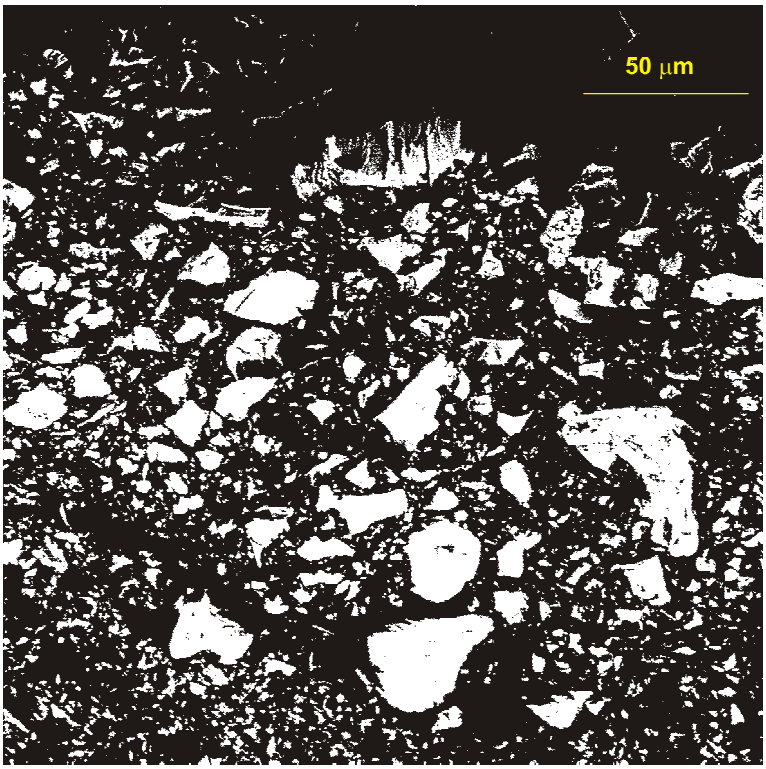

Fig. 2.1b: SEM image of a real sample recorded at the resolution of 2048x2048 pixels.

Changes in average values of morphological parameters of Maximum Feret diameter, perimeter and area, which correspond to all the tested real sample microphotography resolutions (64x64, 128x128, 256x256, 512x512, 1024x1024, and 2048x2048 pixels), are summarized in Fig. 2.2.

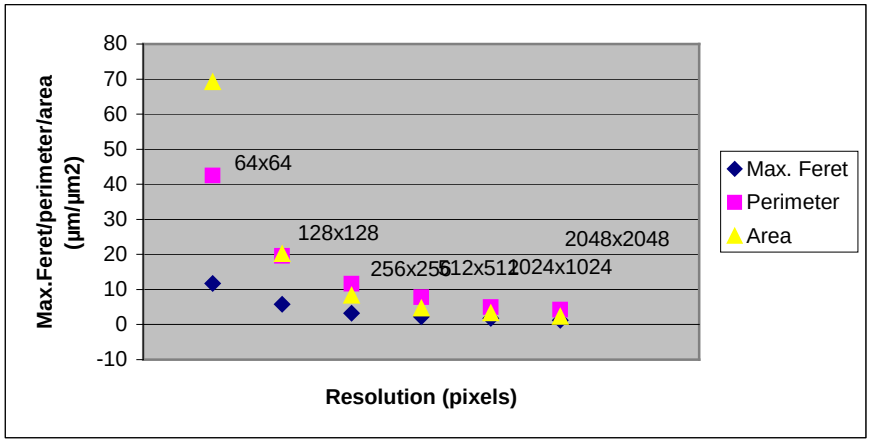

Fig. 2.2: Average values of Maximum Feret diameter, perimeter and area of real sample objects depending on image quality.

As regards particle size, the overall distribution expressed by means of Maximum Feret diameter, the number of particles in the 0-5 micron interval increased with better resolution, whereas the number of particles in all the other size intervals decreased (Fig. 2.3). The difference between the number of detected objects in the 0-5 micron interval at the resolution of 64x64 and 2048x2048 pixels is about 51 %.

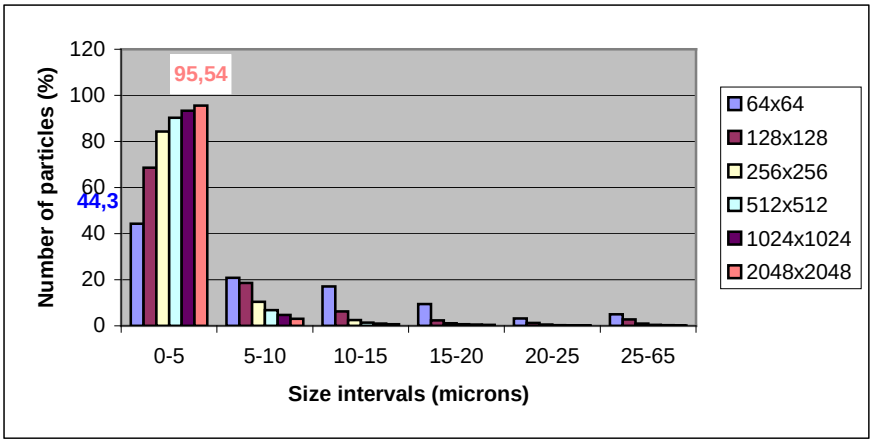

Fig. 2.3: Dependence of real sample particle size distribution on image quality.

2.2. Possible uses of EDX mapping of elements

In addition to the sufficient resolution of the starting image a good threshold setting for the measured objects is also necessary to correctly determine the morphological parameters of particle shape and size. Acquiring an appropriate image, where the phase of interest is well demarcated, may be difficult using light or electron microscopy imaging. Therefore, EDX element mapping, which may be suitable in some cases to demarcate phases of insufficient contrast, was also tested. In order to check and illustrate this procedure the EDX system LINK ISIS (Oxford Instruments) and a sample of a fake painting, „Three Women“ signed “Dominiques”, was used. A photograph of a selected area in the BSE mode is displayed in Fig.2.4a, individual phases lack contrast, therefore, this image is not suitable for processing by image analysis. The following figure, Fig.2.4b, presents an elemental map of the analytical line Hg M alpha 1; in this case the particles containing mercury show a good contrast and are suitable for threshold setting. Fig.2.4c shows an elemental map of Fe K alpha1 line, thanks to which the layer with significant iron contents pigments, which was noticeable in the original figure 2.4a, was successfully highlighted.

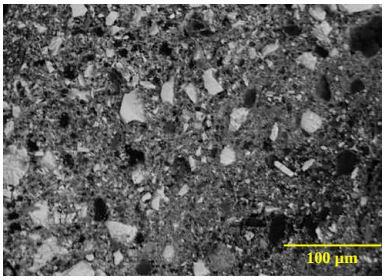

Fig.: 2.4a: Cross-section photography in BSE mode.

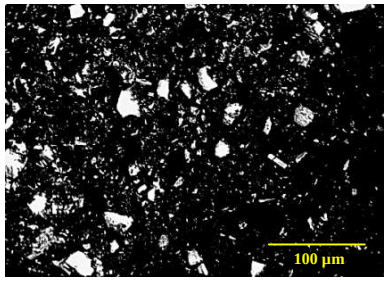

Fig.: 2.4b:Elemental map of Hg M alpha1 line.

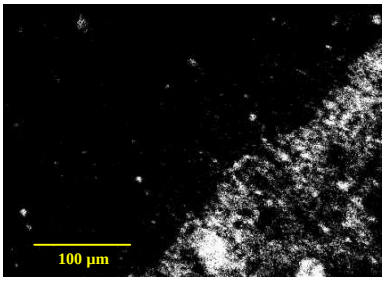

Fig.: 2.4c: Elemental map of Fe K alpha1 line.

Another advantage of elemental maps is that they demarcate only one material phase for eventual statistical evaluation. Elemental map in Fig. 2.4b was used to automatically set threshold for particles containing mercury, for which the average values of selected morphological parameters were subsequently calculated using image analysis software, see Table 2.1.

Table 2.1: Average morphological parameters of mercury containing particles.

Max. Feret (µm)	Min. Feret (µm)	Perimeter (µm)	Circularity	Elongation
1,8815	1,2528	8,865	0,90562	1,4254

2.3. Qualitative and quantitative characterization of selected pigments in real color layers

After performing the tests, morphological parameters of Maximum and Minimum Feret diameter, perimeter, circularity, and elongation were calculated for different artists' pigments from real samples. Common whites and fillers (white lead, barite, and gypsum) and common blues (smalt, azurite, Prussian blue, and indigo) were used. It was documented that measurement is able to distinguish well the different granularity of the same pigment, which often depends on its mode of preparation and required resulting shade of the color. Also, the shape characteristics of pigment granules is related to their origin – precipitated pigments, such as white lead, show higher values of circularity than ground pigments, such as smalt or gypsum. The shape of pigment granules also depends on the physical properties of the pigment, e.g. azurite particles formed by grinding are, thanks to their physical properties, more rounded than particles of smalt, also prepared by grinding, but the fracture of which is sharp, conchoidal. These characteristics may be well quantified using image analysis.

Also, the eventual orientation of particles in the layer is related to their shape and physical properties. It has been found, that cleavable gypsum particles, the elongation of which moves around the value of 2, were oriented in two different directions in the studied layer, which may be related to the way it had been applied. With the help of the correct source image threshold setting and using appropriate logical operations, different kinds of pigment granules in one layer were successfully and automatically distinguished and the morphological parameters for individual pigments were calculated. The image analysis system also made it possible to express the amount of a certain pigment in individual stratigraphy layers as a percentage or calculate the percentual representation of pigments in a mixed layer. To illustrate, an example of granules of different pigments in mixture in one layer of sample M0501-4 is presented (Fig. 2.5).

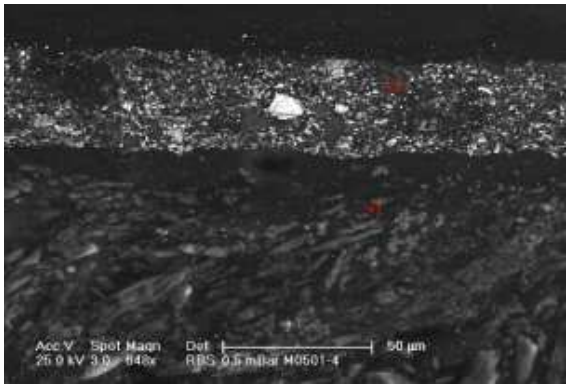

Fig. 2.5: Sample M0501-4 - backscattered electron image.

Layer 2 is a mixture of vermilion, white lead, clays, and particles with high contents of carbon black. Therefore, the aim of the performed measurements was to fully and automatically characterize morphological features of individual pigments of this layer, if possible. Particles of these layers in a SEM microphotograph mutually differ in their shade of gray, therefore, the threshold was set according to the RGB system. In the monochromatic image the brightness level value (interval 0 – 255) was divided into four intervals, by means of which individual pigments were gradually selected:

1) 255-250, which comprises only vermilion particles
2) 255-155, particles of vermilion and white lead
3) 255-90 particles of vermilion, white lead and clays
4) 255-50 in addition to all the previously mentioned particles, this interval also comprised particles with high contents of carbon black with the relatively lowest intensity (Fig. 2.6, 2.7, 2.8, 2.9).

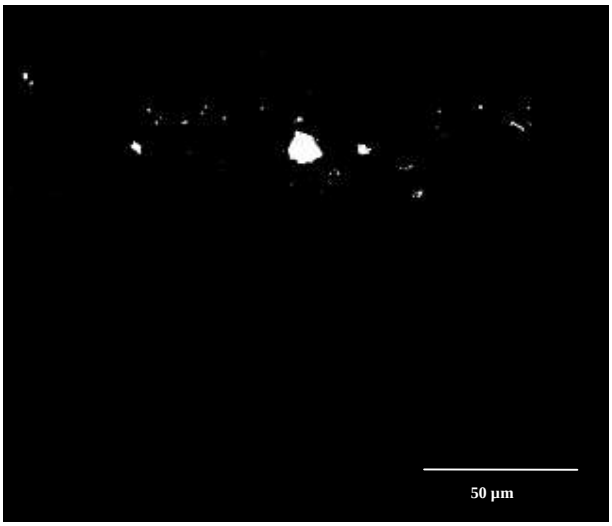

Fig. 2.6: Binary image of vermilion particles corresponding to the intensity range of 255-250 in the M0501-4 sample.

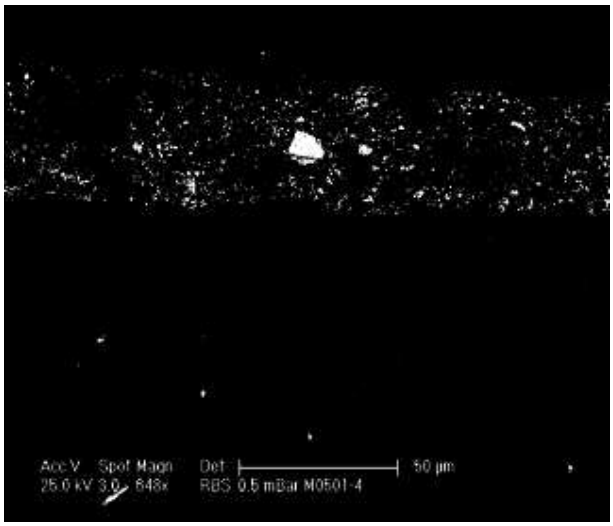

Fig. 2.7: Binary image of particles of vermilion and white lead corresponding to the intensity range of 255-155 in the M0501-4 sample.

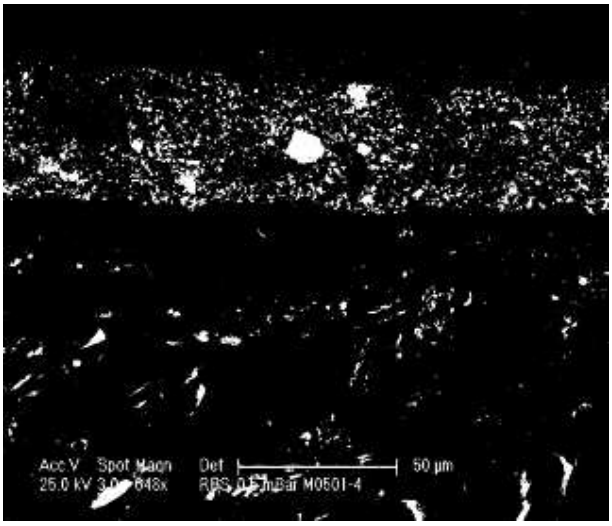

Fig. 2.8: Binary image of particles of vermilion, white lead, and clays corresponding to the intensity range of 255-90 in the M0501-4 sample.

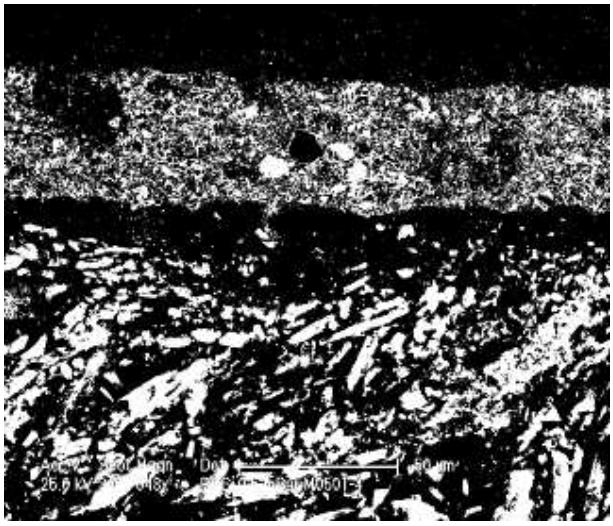

Fig. 2.9: Binary image of particles of vermilion, white lead, clays, and particles with a high contents of carbon black corresponding to the intensity range of 255-50 in the M0501-4 sample.

With appropriate mathematical, morphological, and logical operations with individual binary images, using a mask for layer 2, only particles of the chosen pigment were subsequently selected and, for these, the values of individual features were calculated. The results of morphological features for individual pigments are listed in Table 2.2.

Table 2.2: Selected morphological features characterizing the shape and size of particles of individual pigments in layer 2.

Druh částice	Morphological features				
	Max. Feret (µm)	Min. Feret (µm)	Perimeter (µm)	Circularity	Elongation
Vermilion	1,20850	0,74045	3,29630	0,84321	1,69450
White lead	0,79661	0,47522	2,09910	0,86419	1,65700
Clay	0,70312	0,43835	1,75780	0,92522	1,61740
Particles with a high contents of carbon black	1,80440	1,06200	5,05880	0,69778	1,71660

According to the calculated shape characteristics, it is obvious that the most rounded particles are those of clays, which, at the same time, have the lowest elongation value. In contrast, particles with a high proportion of carbon black show the highest elongation value

and lowest roundness. Shape characteristics of vermilion and white lead are very similar, but white particles are smaller than vermilion particles.

Binary images of individual pigments were used to express the surface representation of different pigments in one layer. Calculated relative representations of different particle types in the mixed color layer No.2 of the M0501-4 sample is represented in Fig. 2.10. Particles with carbon black have the highest surface percentual representation and, in contrast, vermilion particles have the lowest.

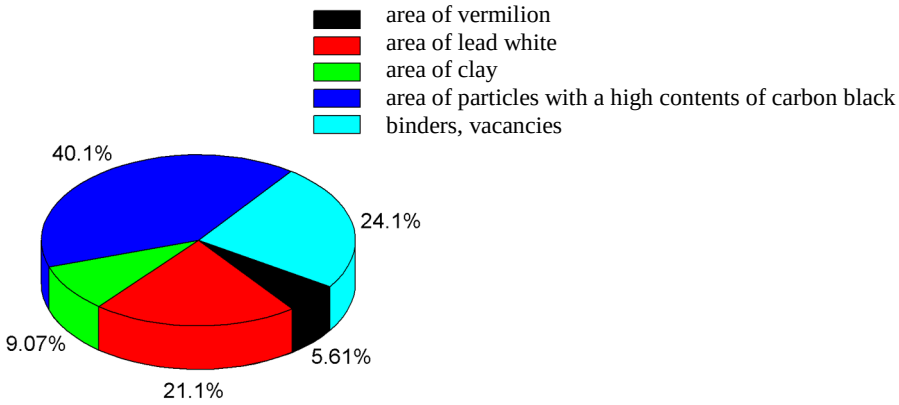

Fig. 2.10: Surface percentual representation of individual pigments in layer 2 of the M0501-4 sample

3. Mobile X-ray fluorescence

The theme of the third focus is linked to the current boom in mobile techniques working *in-situ.* A comparison of two mobile X-ray fluorescence instruments was performed on two selected canvas paintings of the 19th century's so called "Vienna School" circle – „Portrait of Catherine IInd " and the portrait „Maiden in Oriental Dress". The measurements took place right in the Moravian Gallery in Brno.

The results of elemental analysis of almost identical points yielded by both testing instruments were at first compared mutually and, which was the case of „Maiden in Oriental Dress", subsequently compared also with the result of SEM/EDX performed on sampled fragments.

The used X-ray fluorescence devices differed in X-ray tubes and construction. The MOLAB instrument was custom made for the needs of an Italian mobile laboratory MOLAB (W X-ray tube, detector Peltier-cooled detector, detection range according to the manufacturer - Si-U, space resolution of 4 mm at the distance of about 2 cm from the object). The other instrument, X-MET 3000 TX, is produced commercially by Oxford Instruments (Ag X-ray

tube, semiconductor detector, detection range according to the manufacturer - Ti-U, space resolution of 5 mm at the distance of about 4-8 mm from the object).

Different detector resolutions of the compared instruments impact the interpretation of coinciding lines and there are also differences in detection limits. To compare resolution and sensitivity of the assessed mobile XRF analyzers, parts of their measured spectra at 0 - 8.23 keV were superimposed, Fig. 3.1. These regard the analysis of the same area in the portrait „Maiden in Oriental Dress “. The spectrum presented in red was obtained using the MOLAB instrument and the light blue one with the X-MET 3000 TX instrument. The spectra were normalized to Fe.

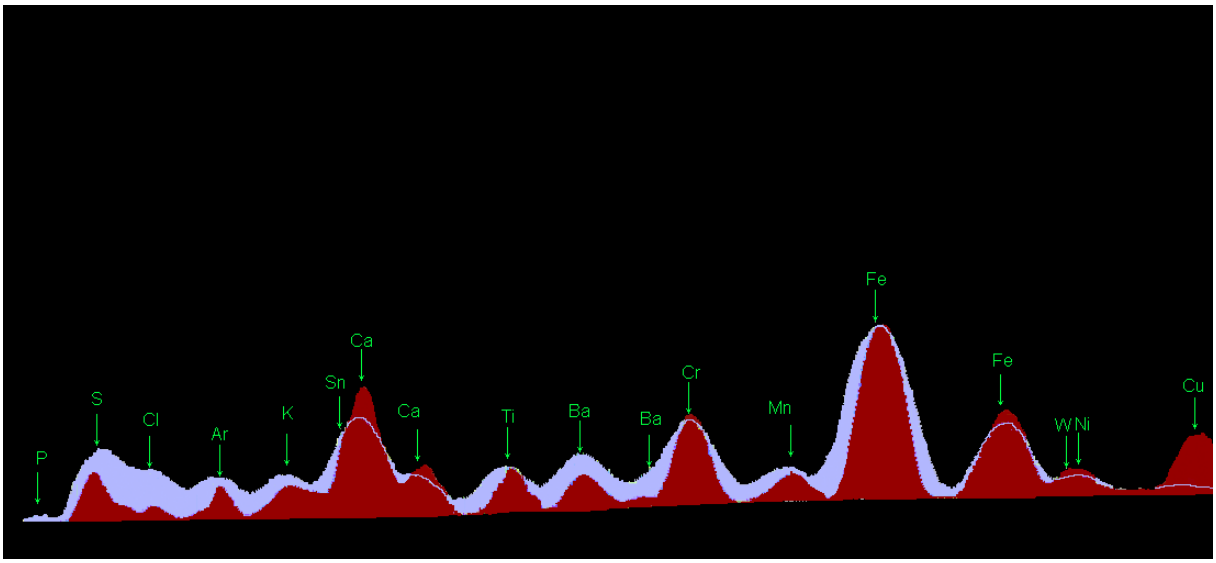

Fig. 3.1.: Graphic comparison MOLAB (red) and X-MET 3000 TX (blue) analyses.

From Fig. 3.1 it is evident that the MOLAB instrument spectrum (red) shows sharper peaks, which is due to better resolution of the detector. This difference is critical, namely in the range of light elements. The commercial XRF device is calibrated for the range of heavy elements, moreover, the detection limit sharply increases towards lighter elements when measuring in the open air. With both instruments, the detection limit for heavy elements in a light matrix is lower than with SEM/EDX. It is possible to identify the same main elements with both instruments. The detection of elements lighter than K (potassium) in the case of mobile XRF, may be generally regarded as questionable. The composition of layers under the surface was diagnosed well, due to the deeper reach of the method under given work conditions.

With regard to its maximum delicacy and the possibility of the reliable identification of main elements in colour layer materials, the Mobile X-ray fluorescence method turned out to be very appropriate for initial screening and selecting areas to take samples for laboratory techniques. From the performed tests it is obvious that laboratory analysis techniques cannot yet be fully replaced by mobile instrument in the field of material research, as the laboratory techniques bring more detailed and exact information not only on phase and quantitative composition, but also on the necessary data concerning stratigraphy of layers of the artwork.

Pigments, minerals and other phases discussed in the summary

Albite	$NaAlSi_3O_8$
Calcite	$CaCO_3$
Carbon black	C
Celadonite	$K(Mg,Fe)(Fe,Al)Si_4O_{10}(OH)_2$
Cerusite	$CaCO_3$
Clay (ochre)	Yellow ochre, $Fe_2O_3 \cdot H_2O$, a hydrated iron oxide Red ochre, Fe_2O_3, the anhydrate of yellow ochre, which turns red when heated, as this drives off the water ligands. Brown ochre (Goethite), also partly hydrated iron oxide (rust)
Gypsum	$CaSO_4 \cdot 2H_2O$
Hematite	Fe_2O_3
Chlorite	(Fe, Mg, Al)6(Si, A;l)4O10(OH)8, Iron Aluminum Magnesium Silicate Hydroxide
Kaolinite	$Al_2Si_2O_5(OH)_4$
Quartz	SiO_2
Vermilion	HgS
White lead	$2PbCO_3 \cdot Pb(OH)_2$